Chemical Engineering Journal 151 (2009) 39–45

Contents lists available at ScienceDirect

Chemical Engineering Journal

journal homepage: www.elsevier.com/locate/cej

Numerical investigation of performance characteristics of a cyclone prolonged with a dipleg

Fuat Kaya *, Irfan Karagoz [1]

Uludag University, Department of Mechanical Engineering, 16059 Bursa, Turkey

ARTICLE INFO

Article history:
Received 23 May 2008
Received in revised form 19 January 2009
Accepted 26 January 2009

Keywords:
Swirling flows
Separation efficiency
Numerical simulation
Lagrangian method

ABSTRACT

Numerical modeling of a particle separation process is carried out to understand the gas-particle two-phase flow field inside a cyclone prolonged with a dipleg and results of the numerical simulations are compared with experimental data to validate the numerical results. The flow inside the cyclone separator is modeled as a three-dimensional turbulent continuous gas flow with solid particles as a discrete phase. The continuous gas flow is predicted by solving Navier–Stokes equations using the differential RSM turbulence model with nonequilibrium wall functions. The second phase is modeled based on a Lagrangian approach. Analysis of computed results shows that the length of the dipleg considerably influences the cyclone separation efficiency rather than the cyclone pressure drop, especially for lower inlet velocities in relatively short cyclones, by providing more separation space.

1. Introduction

An efficient removal of particles from two-phase flows is essential to develop advanced separation technologies. Cyclone separators are widely used for this purpose, due to their several advantages such as simple design, absence of moving parts, low manufacturing and maintenance costs. Entrance of flow into cyclone can be axial or tangential through inlet section, which can be in different shapes for each cyclone. Cyclone separators operate under the action of centrifugal forces. Fluid mixture enters the cyclone and makes a swirl motion and, due to the centrifugal forces, the particles in the flow gain a relative motion in the radial direction and are separated from the main flow. It is difficult to analyze this problem, since this swirling flow is very complex, and there are many parameters influenced this flow. The main performance characteristics of a cyclone separator are collection efficiency, fractional efficiencies and pressure losses. Many experimental and theoretical studies performed on this difficult problem provide semiempirical models ranging from simple [1–4] to more comprehensive models [5,6] for the prediction of a cyclone performance.

Due to the fact that the fluids dynamics of cyclones are complex, including highly turbulent structure and limitations in the usage of empirical models, optimization of cyclone performance by improving the cyclone efficiency and minimizing the pressure drop was essentially based on experiments rather than theoretical studies [7–14]. However, the computational fluid dynamics (CFD) of cyclones has exploded recently with advances in computer capabilities, numerical methods and software, and with the advent to the field of a large number of investigators [15–23].

Although many works have been carried out to investigate the influence of different geometric parameters such as cyclone length, inlet and outlet pipe geometries etc. on the performance of cyclones, there has been little work concerning the dust outlet geometries. Obermair et al. [24] performed cyclone tests with five different dust outlet geometries to find the influence of the dust outlet geometry on the separation process. They showed that separation efficiency can be improved significantly by changing the dust outlet geometry, and they reported that further research is needed to clarify precise effects of dust outlet geometry. The effect of a dipleg was posed and investigated by several researchers [25–27].

It is well known that in a reverse flow cyclone, the outer vortex flow weakens and changes its direction at a certain axial distance from the vortex finder. This axial magnitude has been called the “natural length” or the “vortex length” of the cyclone, and the axial position is referred to as “the end of the vortex”. The influence of the dipleg on the vortex and flow characteristics was investigated by Gil et al. [27], and they found that the vortex end was related not only to inlet and vortex finder geometry, but also to inlet gas velocity and solid loading. They also found that a small amount of “underflow” drawn through the dust exit causes the vortex end to move down the dipleg and a higher dust loading caused the end of the vortex to move up the dipleg.

Hoffmann et al. [28] studied the effect of cyclone length on separation efficiency and pressure drop, experimentally and theoretically, by varying the length of the cylindrical segment of a cylinder-on-cone cyclone. They showed that the separation efficiency improves for certain ratio of L/D. However, they found an

* Corresponding author. Tel.: +90 224 2941997; fax: +90 224 2941903.
E-mail address: fkaya@uludag.edu.tr (F. Kaya).
[1] Tel.: +90 224 2941911; fax: +90 224 2941903.

1385-8947/$ – see front matter © 2009 Elsevier B.V. All rights reserved.
doi:10.1016/j.cej.2009.01.040

optimal cyclone length: lengthening the cyclone to more than $L/D = 5.65$ dramatically lower separation efficiency.

Qian et al. [29] studied, experimentally and numerically, a cyclone prolonged with a dipleg. They stated that the dipleg has important influence on separation efficiency of the cyclones. However, their work is very specific and has not exhaustively explored the effects of the dipleg. They studied only one cyclone with three different dipleg lengths. Their experimental and numerical tests were carried out for a single inlet velocity and a particle diameter, respectively. Therefore, the question can be considered still open and needs further investigation.

The aim of the present study is to give a detailed description of the flow structure in a tangential inlet cyclone with a dipleg located under the cyclone and to investigate the effects of the dipleg on the cyclone collection efficiency and pressure drop. Computational results were verified by comparing them with experimental data available in the literature. The differential Reynolds Stress Model (RSM) was employed for turbulence closure and the Lagrangian approach was used to compute discrete particle motions.

2. Theoretical bases

2.1. Modeling of airflow and turbulence

Cyclone separator consists of three main parts: inlet, separation chamber and vortex finder. Tangential inlets are preferred for the separation of particles from gases [30]. Therefore, the present work is deal with a tangential inlet cyclone whose schematic representation is given in Fig. 1.

The Reynolds-averaged equations for conservation of mass and momentum can be written in the following compact form:

$$\frac{\partial(\rho\phi)}{\partial x_t} + \frac{\partial(\rho u_j \phi)}{\partial x_j} = \frac{\partial}{\partial x_j}\left[\Gamma_\varphi \frac{\partial \phi}{\partial x_j}\right] + S_\varphi \tag{1}$$

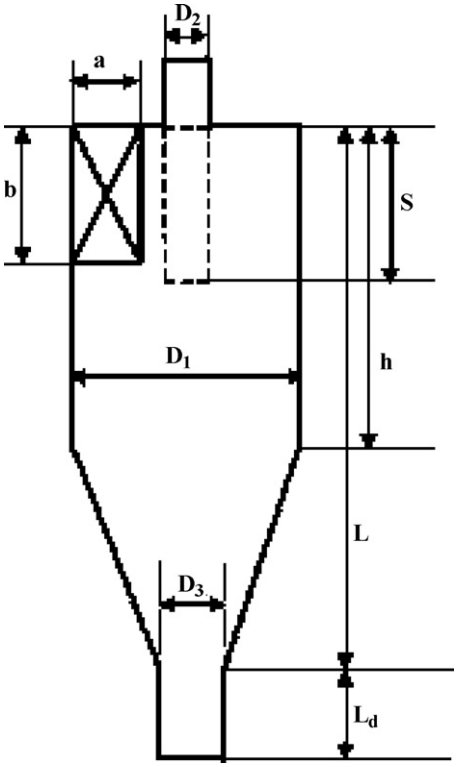

Fig. 1. Tangential inlet cyclone.

where ϕ is a universal dependent variable, Γ_φ is the diffusivity, and S_φ is the source term. For the continuity equation, ϕ is l, Γ_φ and S_φ are 0. In the momentum equations, ϕ, Γ_φ, and S_φ stand for u_i, μ and

$$-\frac{\partial P}{\partial x_i} + \rho g_i + \frac{\partial}{\partial x_j}\left(\mu\frac{\partial u_i}{\partial x_j} - \frac{2}{3}\delta_{ij}\frac{\partial u_l}{\partial x_l}\right) - \frac{\partial}{\partial x_i}(\rho\overline{u_i' u_j'})$$

respectively.

In order to obtain values for the Reynolds stress terms ($\rho\overline{u_i' u_j'}$), the differential Reynolds stress model (RSM) was used, due to strong anisotropy in the cyclone flow. The RSM closes the governing equations by solving transport equations for individual Reynolds stresses as

$$\frac{\partial \rho\overline{u_i u_j}}{\partial t} + \frac{\partial}{\partial x_k}\left(U_k \partial \rho\overline{u_i u_j}\right) = P_{ij} + \phi_{ij} + \frac{\partial}{\partial x_k}\left[\left(\mu + \frac{2}{3}c_s\rho\frac{k^2}{\varepsilon}\right)\frac{\partial \rho\overline{u_i u_j}}{\partial x_k}\right] - \frac{2}{3}\delta_{ij}\varepsilon\rho \tag{2}$$

where $P_{i,j}$ is the production term, and ϕ_{ij} is the pressure–strain correlation term. The pressure–strain correlation term is responsible for the redistribution of turbulent energy amongst the six stress components and needs modeling. The linear pressure–strain model was used to model this term [31].

The turbulence dissipation (ε) appears in the individual stress equations and can be expressed as

$$\frac{\partial \rho\varepsilon}{\partial t} + \nabla\cdot(\rho U\varepsilon) = \frac{\varepsilon}{k}(c_{\varepsilon 1}P - c_{\varepsilon 2}\rho\varepsilon) + \nabla\cdot\left[\frac{1}{\sigma_{\varepsilon RS}}\left(\mu + \rho C_{\mu RS}\frac{k^2}{\varepsilon}\right)\nabla\cdot\varepsilon\right] \tag{3}$$

The model constants in these equations are $c_s = 0.22$, $c_{\varepsilon 1} = 1.45$, $c_{\varepsilon 2} = 1.9$, $C_{\mu RS} = 0.1152$.

2.2. Modeling of particle motion

Modeling of particle motion is based on the assumptions that the second phase consists of spherical particles dispersed dilutely in the continuous phase so that particle–particle interactions and effect of the particle volume fraction on the continuous phase are negligible. In this study, the discrete phase model (DPM) was used to simulate the second phase in a Lagrangian frame of reference by defining the initial position, velocity and size of individual particles.

The trajectory of a particle was obtained by integrating the force balance on the particle. This force balance equates the particle inertia with the forces acting on the particle and can be written in the following form:

$$\frac{du_p}{dt} = F_D(u - u_p) + \frac{g(\rho_p - \rho)}{\rho_p} + F_x \tag{4}$$

where $F_D(u - u_p)$ is the drag force per unit particle mass and can be written as [31]

$$F_D = \frac{18\mu}{\rho_p d_p^2}\frac{C_D Re_r}{24} \tag{5}$$

Re_r is the relative Reynolds number, which is defined as

$$Re_r = \frac{\rho d_p |u_p - u|}{\mu} \tag{6}$$

where u is the fluid phase velocity, u_p is the particle velocity, μ is the molecular viscosity of the fluid, ρ is the fluid density, ρ_p and d_p are the density and the diameter of the particle, respectively. The drag coefficient C_D for spherical particles is calculated by using the correlation developed by Morsi and Alexander [32].

F_x denotes additional forces such as Brownian forces, thermophoretic forces, acceleration forces etc., per unit particle mass. These forces may be important depending on the flow and operational conditions. More information can be found in related literature [31].

3. Numerical method

Governing equations were solved numerically by using finite volume based Fluent CFD code. According to the basic idea of the control volume method, the computation domain is divided into a number of cells, and the differential equation is integrated over each cell to obtain the corresponding discretized equations. These algebraic equations were solved iteratively to obtain the field distribution of dependent variables. The Presto interpolation scheme for pressure, the Simplec algorithm for pressure–velocity coupling and the quadratic upstream interpolation for convective kinetics (Quick) scheme for momentum variables were used giving satisfactory results for highly swirling flows in cyclones. Due to difficulty to reach the convergence in simulations, the first order upwind scheme was applied for discretization of the Reynolds stresses. Details on these schemes can be found in the literature.

The boundary condition for airflow velocities at the cyclone inlet was assumed to be uniform at different inlet velocities. The outflow boundary condition was used at the exit. At the walls, no slip boundary condition was applied for velocity, and near-wall treatment was achieved by using nonequilibrium wall functions.

Extensive grid refinement tests have been done on the flow fields of cyclone so as to get grid independent solution. Typical computational meshes are shown in Fig. 2 for the cyclones C1 and C2, with and without a dipleg. Numerical experiments were carried out with the residuals less than 10^{-5}.

4. Results and discussion

The particulate flow structure in a tangential inlet cyclone and the effects of the dipleg length on the cyclone performance were investigated by using Fluent CFD code. The differential Reynolds Stress model with nonequilibrium wall function was used to model turbulence, and the Discrete Phase Model was applied to simulate particle motion. Predicted results were validated by comparing them with the experimental values given in the literature [14]. Operating conditions (such as flow rate, dust loading, temperature, pressure, density) in numerical simulations have been taken as in the related references. Three cyclones, different in type and size, have been tested in this study. The dimensions of them are given in Table 1. The second cyclone (C2) is the Stairmand high efficiency cyclone.

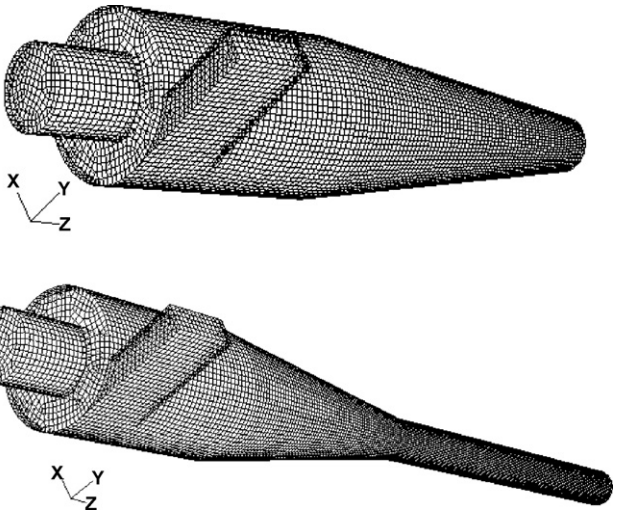

Fig. 2. CFD surface mesh for the cyclone with and without a dipleg.

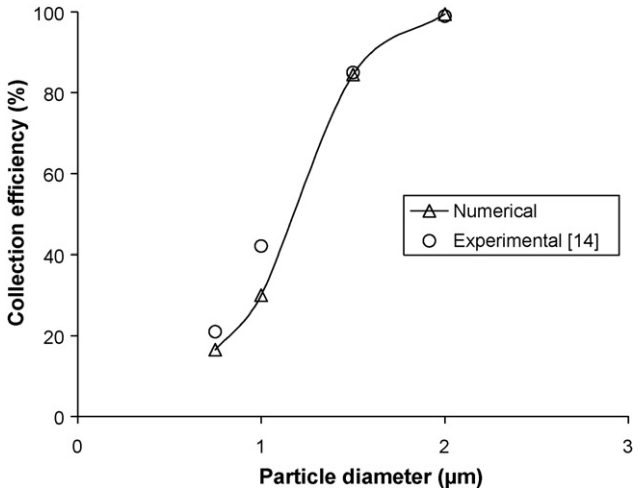

Fig. 3. Comparison between computed particle collection efficiency and experimental data (V_i = 16 m/s).

All numerical solutions were obtained with the particle diameters between 0.75 and 3 μm, and the inlet velocity (V_i) was changed between 7 and 19 m/s. The lengths of the dipleg tested in the simulations are L_d/L = 0 (without dipleg), 0.5, and 1, denoted as A, B, and C cyclones, respectively. Figs. 3 and 4 give the comparisons between the computed efficiency and experimental data for the inlet velocities of 16 and 8 m/s in the cyclone C1 without dipleg, respectively. The curve for the computed cyclone efficiency has the S shape and agrees well with the experimental data. The difference between the predicted efficiency and the experimental data is less than 7%.

The pressure drop and particle cut-off size computed in the cyclone C3 are compared with the experimental values as well as with the CFD results given in the literature [28] in Table 2 for the inlet velocity of 19 m/s. The results computed in the present study show better agreement with the experimental values than the computed results given in the literature, especially for pressure drop.

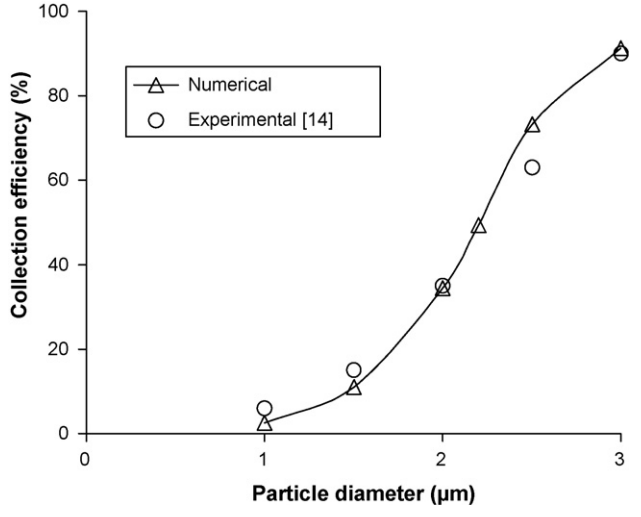

Fig. 4. Comparison between computed particle collection efficiency and experimental data (V_i = 8 m/s).

Table 1
Geometrical dimensions of the cyclones used in this study.

Model	a (mm)	b (mm)	D_2 (mm)	S (mm)	h (mm)	L (mm)	D_3 (mm)	D_1 (mm)
C1	5	12.5	15.5	15.5	31	77	11.6	31
C2 (Stairmand)	4	10	10	10	30	80	7.5	20
C3	50	114	65	140	260–560–960	670–970–1370	110	200

Table 2
Comparison of the computed results with experimental values for the cyclone C3.

	Pressure drop (Pa)	Cut-off size (μm)
Experimental [28]	3600	1.15
CFD [28]	3000	2.1
Present CFD	3601	1.66

After these validation studies, different dipleg lengths were modeled and the role of the dipleg on the flow structure and the cyclone performance were investigated in detail.

4.1. Velocity fields of conventional and prolonged cyclones

Tangential and axial velocities are two important variables of the gas flow in a cyclone. Tangential velocity creates centrifugal forces needed for particle separation. Axial velocity makes particle transport to the dustbin. The tangential velocity contours and velocity profiles of the conventional and prolonged cyclones are presented in Figs. 5 and 6 for the inlet velocity of 16 m/s, in the cyclone C1.

The simulation results show that the length of the dipleg has a negligible influence on the tangential velocity distribution in the cylindrical part. Although the maximum tangential velocities almost remain the same and a small decrease is observed with the increasing of the dipleg length in the core of the conical part, an increased dipleg length results in a reduced tangential velocity in the dipleg (Fig. 5). However, the tangential velocity relatively high over the entire length of the dipleg for L_d = 38.5 compare to the longest dipleg. This also indicates that the vortex does not attain to the bottom for the longest dipleg. Fig. 6 also shows the decrease in the tangential velocity profiles along radius at the same position from the bottom (z = 0.076, 0.1145 and 0.153 m).

Fig. 7 shows the static pressure contours in the cyclone C1, for V_i = 7 m/s. The decrease in the pressure values toward bottom of the

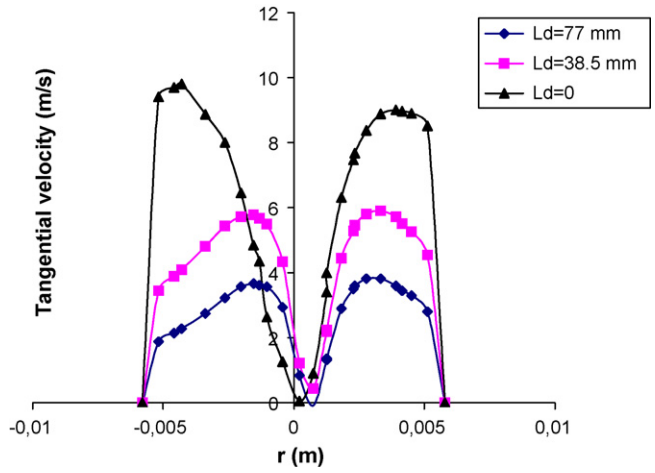

Fig. 6. Tangential velocity profiles along the radius, position at z = 0.076 m, 0.1145 m and 0.153 m (V_i = 16 m/s, C1).

dipleg is caused by the low tangential velocities below the vortex end. For the longest dipleg, a nearly constant radial pressure at the lower part of the dipleg indicates the presence of the vortex end location.

As can be seen from Figs. 8–10, the dipleg length considerably influences the axial velocity distribution. Two flow regions are clear. Along the wall, a vortex moves down and transports the centrifuged particles, and a second vortex moves upwards in the center. Figs. 9 and 10 compare the axial velocity profiles quantitatively at the sections in the cylindrical (z = 0.03 m) and in the conical (z = 0.053 m) parts, respectively. The effect of the dipleg is negligible in the outer vortex; however, when the dipleg length is increased, two-peak shape axial velocity profile in the core disappears and upward velocity increases. This increase in upward velocity is pro-

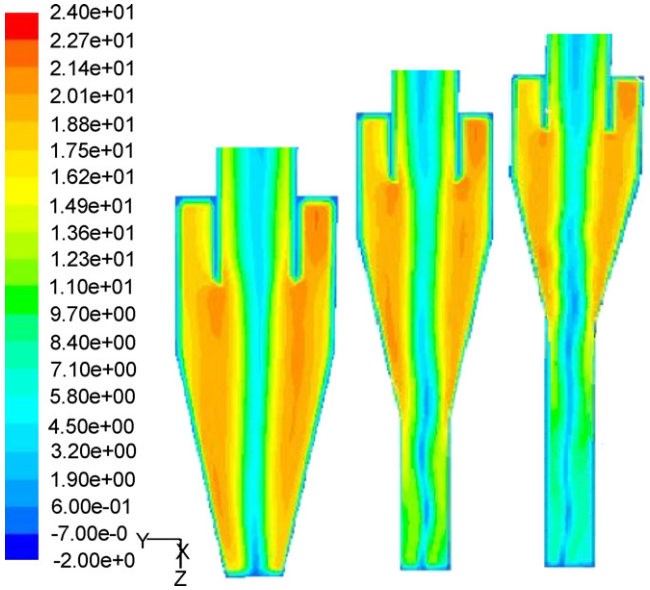

Fig. 5. Tangential velocity contours of the cyclones A, B, C (V_i = 16 m/s, C1).

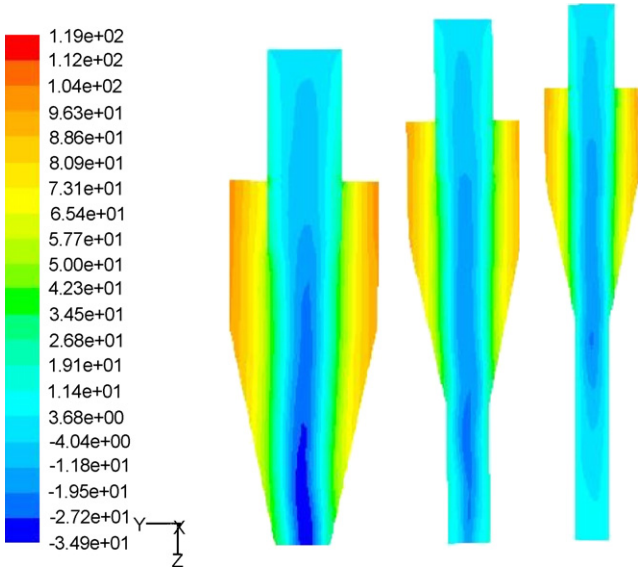

Fig. 7. Static pressure contours of the cyclones A, B, C (V_i = 7 m/s, C1).

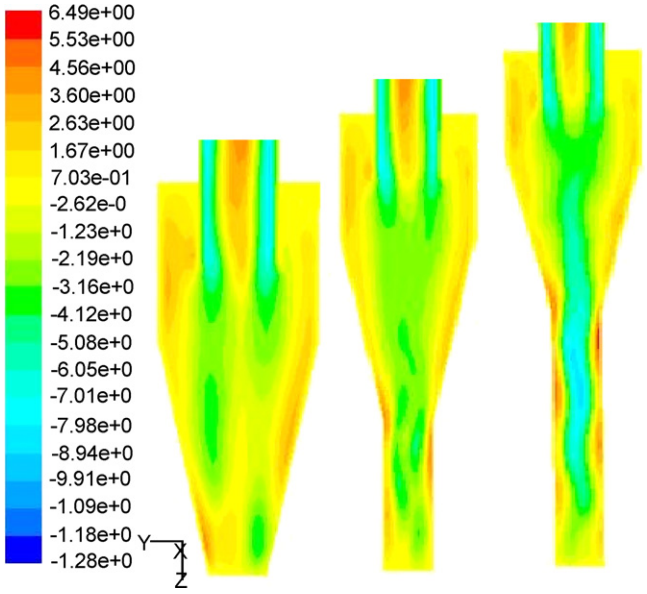

Fig. 8. Axial velocity contours of the cyclones A, B, C (V_i = 16 m/s, C1).

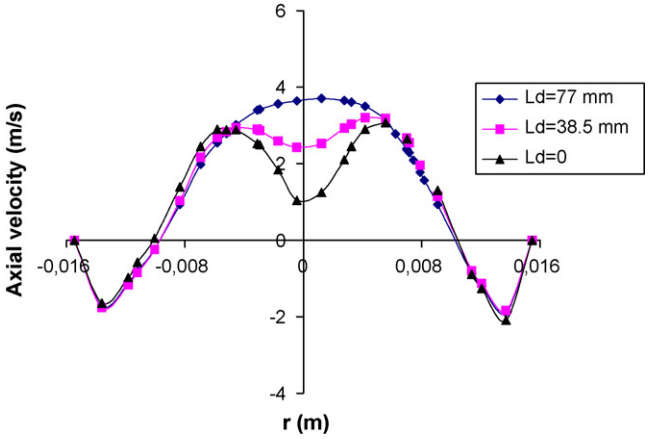

Fig. 9. Comparison of axial velocity profile computed at different dipleg lengths (z = 0.03 m, V_i = 16 m/s).

moted by shortcut flows into the inner vortex. Similar behavior is observed for the variation of turbulent kinetic energy (Fig. 11). As expected, the size of the low turbulent kinetic energy region at the bottom of the cyclone increases with the increase in the dipleg length. However, at the conical part, the turbulent kinetic energy becomes minimum value when the dipleg length is about 38 mm. Therefore, one can expect that the lower turbulent kinetic energy in

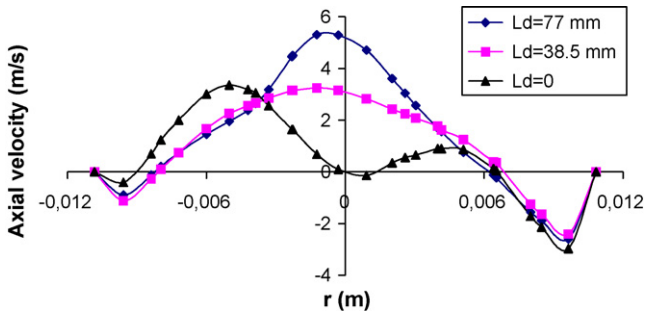

Fig. 10. Comparison of axial velocity profile computed at different dipleg lengths (z = 0.053 m, V_i = 16 m/s).

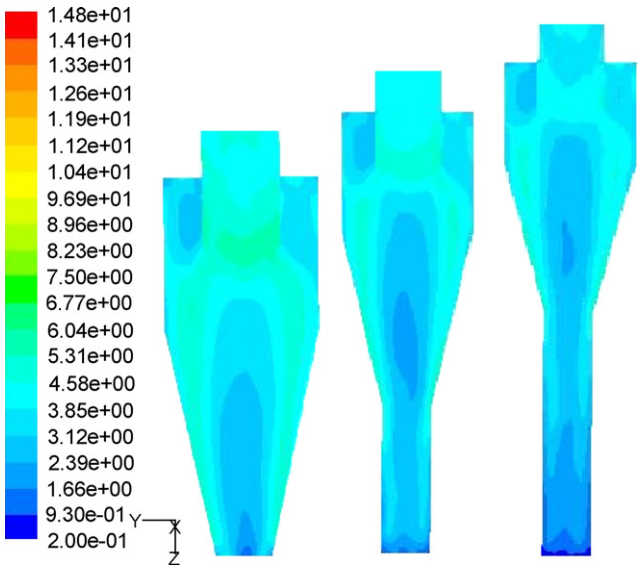

Fig. 11. Contours of turbulent kinetic energy of cyclone (V_i = 16 m/s).

the conical part will prevent the entrainment of particles and will improve the separation process.

4.2. Performance analysis of conventional and prolonged cyclones

Fig. 12 shows the fractional efficiency curves for different dipleg lengths in the cyclone C1 for the inlet velocity of 8 m/s. The length of the dipleg considerably affects the fractional efficiency. The prolonged cyclone can provide more separation space, which is useful to increase the separation efficiency. However, results obtained from the numerical tests for all velocities and particle diameters have demonstrated that the best efficiency was obtained for the dipleg length of 38.5 which corresponds the half of the cyclone height. The main reason might be the natural vortex length. In the case of L_d = 38.5 mm, the vortex end reaches the bottom of the dipleg leads to a high collection efficiency. Further increase in the dipleg length makes the vortex shorter. In this case, the vortex end attaches to the wall and crates instabilities which eventually cause re-entrainment of separated particles and low efficiency; the same effect was found with higher solids loadings in cyclones [27]. On the other hand, relatively lower turbulence kinetic energy is seen in the conical part, which may assist improving efficiency.

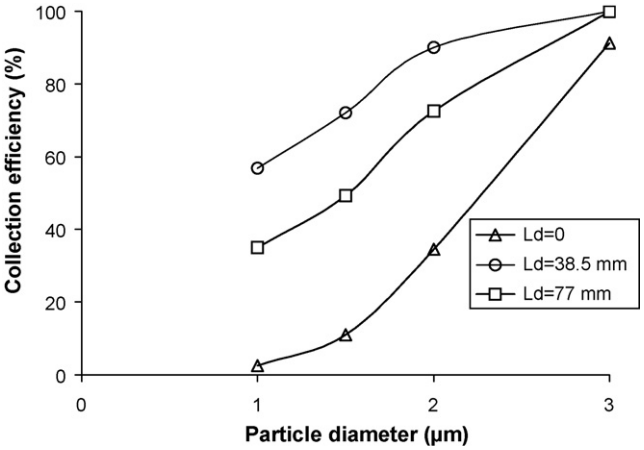

Fig. 12. Comparison of fractional efficiency computed at different dipleg lengths in C1 (V_i = 8 m/s).

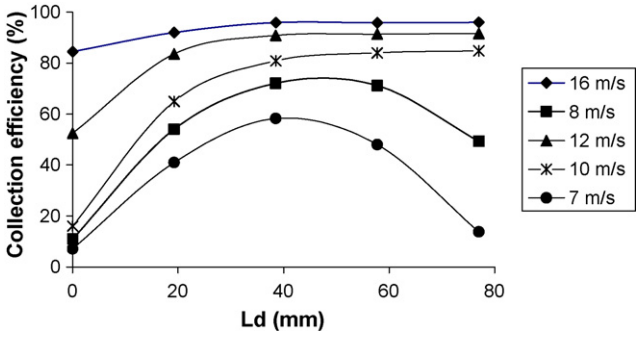

Fig. 13. Comparison among the particle collection efficiencies of the prolonged C1 cyclones for different inlet velocities (d_p = 1.5 μm).

The computed efficiencies under five different inlet velocities are shown in Figs. 13 and 14 for particle diameters of 1.5 and 2 μm, respectively. A clear trend of increasing collection efficiency is seen up to the length of about 40 mm in the cyclone C1 (Figs. 13 and 14). However, the efficiency starts to decrease for the inlet velocities lower than 10 m/s which corresponds to the inlet Reynolds number of about 10^4, and remains almost the same for the higher velocities. These figures also show that collection efficiency is increasing with the increase of inlet velocity for all particle diameters at any length of dipleg. Higher particle diameter also leads to higher collection efficiency, as expected. The optimal dipleg length is obtained at about $L_d/L = 0.5$ for the cyclone C1 which is shorter than the conventional Stairmand high efficiency cyclone without dipleg. As can be seen from Fig. 14, the Stairmand high efficiency cyclone (C2) does not exhibit higher collection efficiency when the dipleg length increases. The main reason is that the Stairmand high efficiency cyclone has an optimal length ($L/D = 4$). Therefore, further increase in the length by using a dipleg may cause a decrease in efficiency. Numerical tests with larger cyclones were also carried out. The results of the cyclone with a diameter of 200 mm (C3) have been also included in Fig. 14. The effect of the dipleg length is not significant for this cyclone. The inlet Reynolds number is bigger than 3×10^4 due to larger inlet hydraulic diameter and L/D is about 3.35 for this cyclone. Therefore, the results from these tests showed negligible influence of the dipleg length on the collection efficiency. Similar trend was also observed for the other particle diameters.

Although the dipleg length considerably influences the collection efficiency, its effect on the cyclone pressure drop is negligible. By increasing the length of dipleg, the surface for wall friction is increased, which should result in a lower tangential velocity. Therefore, a small decrease is observed as the dipleg length increases for higher inlet velocities, and pressure drop in the cyclone almost

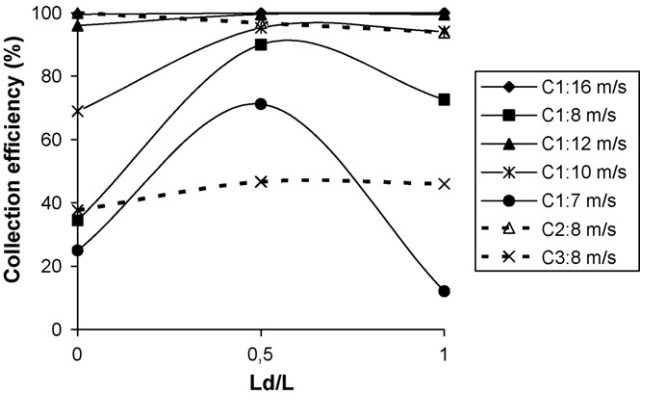

Fig. 14. Comparison among the particle collection efficiencies of the prolonged cyclones for different inlet velocities (d_p = 2 μm).

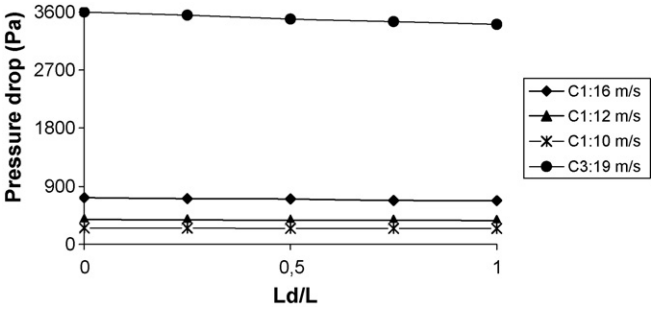

Fig. 15. Comparison among the pressure drop of the prolonged cyclones for different inlet velocities.

remains the same for lower velocities, as can be seen in Fig. 15. Increasing in the inlet velocity also causes an increase in pressure drop.

5. Conclusion

This study is deal with the numerical investigation of isothermal flow characteristics and particle collection efficiencies of conventional and prolonged cyclones. The results computed by using the differential RSM turbulence model were validated with the experimental values given in the literature. The collection efficiency and pressure drop were evaluated for various dipleg lengths at different inlet velocities and particle diameters.

It is concluded from the results that the separation efficiency can be improved by using a dipleg which leads to a change in flow pattern, for tangential inlet short cyclones. The tangential velocity and turbulence in these cyclones are reduced by a longer dipleg. However, an excessive increase in the dipleg length leads the upward axial velocity to increase in the core region, due to vortex turning.

The static pressure values decrease toward the bottom of the dipleg due to low tangential velocities and become nearly constant in radial direction, where there is very low swirl, showing the existence of the vortex end location, especially for longer dipleg.

By increasing the length of the dipleg, the surface for wall friction is increased, which should results in a slightly lower tangential velocity. This eventually causes less pressure drop especially at high inlet velocities.

The length of the dipleg influences the cyclone performance considerably in cyclones shorter than the Stairmand high efficiency cyclone. The fractional separation efficiency increases up to a certain level depending on particle diameter by increasing the length of the dipleg, due to increase of separation space. Further increase in dipleg length may cause the separation efficiency to decrease especially at the inlet velocities lower than 10 m/s which corresponds to the inlet Reynolds number of about 10^4, and remains almost the same for the higher velocities. A decrease in cone, and therefore, dipleg diameter leads to slightly higher collection efficiency and pressure drop. However, the effects of the dipleg length do not change with the cone dimensions.

References

[1] G.B. Shepherd, C.E. Lapple, Flow pattern and pressure drop in cyclone dust collectors, Ind. Eng. Chem. 31 (1939).
[2] R.M. Alexander, Fundamentals of cyclone design and operation, Proc. Aus. Inst. Min. Met. NS 152–153 (1949) 203–228.
[3] W. Barth, Berechnung und Auslegung von Zyklonabscheiden auf Grund neuerer Untersuchungen, BWK 8 (1956) 1–9.
[4] W. Barth, L. Leineweber, Evaluation of design of cyclone separators, Staub. Reinhalt. Luft 24 (1964) 41–55.
[5] A. Avci, I. Karagoz, Effect of flow and geometrical parameters on the collection efficiency incyclone separators, J. Aerosol Sci. 34 (2003) 937–955.
[6] I. Karagoz, A. Avci, Modelling of the pressure drop in tangential inlet cyclone separators, Aerosol Sci. Technol. 39 (2005) 857–865.

[7] M.E. Moore, A.R. Mcfarland, Performance modelling of single-inlet aerosol sampling cyclones, Environ. Sci. Technol. 27 (1993) 1842–1848.
[8] L.C. Kenny, R.A. Gussman, Characterizations and modelling of a family of cyclone preseparators, J. Aerosol Sci. 26 (1995) 777–778.
[9] C.J. Stairmand, The design and performance of cyclone separators, Trans. Inst. Chem. Eng. 29 (1951) 356–383.
[10] C.E. Lapple, Processes use many collector types, Chem. Eng. 58 (1951) 144–151.
[11] J.C. Kim, K.W. Lee, Experimental study of particle collection by small cyclones, Aerosol Sci. Technol. 12 (1990) 1003–1015.
[12] C. Köning, H. Büttner, F. Ebert, Desing data for cyclones, Particle and particle systems characterization 8 (1991) 301–307.
[13] S.L. Upton, D. Mark, W.D. Griffiths, A wind tunnel evaluation of the sampling efficiencies of three bioaerosol samplers, J. Aerosol Sci. 25 (1994) 1493–1501.
[14] R. Xiang, S.H. Park, K.W. Lee, Effects of cone dimension on cyclone performance, J. Aerosol Sci. 32 (2001) 549–561.
[15] J. Gimbun, T.G. Chuah, A. Fakhru'l-Razi, S.Y. Choong Thomas, The influence of temperature and inlet velocity on cyclone pressure drop: a CFD study, Chem. Eng. Process. 44 (2005) 7–12.
[16] A.J. Hoekstra, J.J. Derksen, H.E.A. Van Den Akker, An experimental and numerical study turbulent swirling flow in gas cyclones, Chem. Eng. Sci. 54 (1999) 2055–2065.
[17] A.L. Gong, L.Z. Wang, Numerical study of gas phase flow in cyclones with the repds, Aerosol Tech. 38 (2004) 506–512.
[18] T.G. Chuah, J. Gimbun, S.Y. Choong Thomas, A CFD study the effect of cone dimensions on sampling aerocyclones performance and hydrodynamics, Pow. Technol. 162 (2006) 126–132.
[19] L. Ma, D.B. Ingham, X. Wen, Numerical modelling of the fluid and particle penetration through small sampling cyclones, J. Aerosol Sci. 31 (2000) 1097–1119.
[20] D.B. Ingham, L. Ma, Predicting the performance of air cyclones, Int. J. Eng. Res. 26 (2002) 633–652.
[21] I. Karagoz, F. Kaya, CFD investigation of the flow and heat transfer characteristics in a tangential inlet cyclone, Int. Commun. Heat Mass Transf. 34 (2007) 1119–1126.
[22] J.J. Derksen, H.E.A. Van den Akker, S. Sundaresan, Two-way coupled large-eddy simulations of the gas–solid flow in cyclone separators, AIChE J. 54 (2008) 872–885.
[23] F. Kaya, I. Karagoz, Performance analysis of numerical schemes in swirling turbulent flows in cyclones, Curr. Sci. 94 (2008) 1273–1278.
[24] S. Obermair, J. Woisetschlager, G. Staudinger, Investigation of the flow pattern in different dust outlet geometries of a gas cyclone by laser Doppler anemometry, Pow. Technol. 138 (2003) 239–251.
[25] A.C. Hoffmann, M. De Groot, A. Hospers, The effect of the dust collection system on the flowpattern and separation efficiency of a gas cyclone, Can. J. Chem. Eng. 74 (1996) 464–470.
[26] C. Cortes, A. Gil, Modeling the gas and particle flow inside cyclone separators, Progr. Eng. Comb. Sci. 33 (2007) 409–452.
[27] A. Gil, C. Cortes, L.M. Romeo, J. Velilla, Gas-particle flow inside cyclone diplegs with pneumatic extraction, Pow. Technol. 128 (2002) 78–91.
[28] A.C. Hoffmann, M. De Groot, W. Peng, H.W.A. Dries, J. Kater, Advantages and risks in increasing cyclone separator length, AIChE J. 47 (11) (2001) 2452–2460.
[29] F. Qian, J. Zhang, M. Zhang, Effect of the prolonged vertical tube on the separation performance of a cyclone, J. Hazar. Mater. B136 (2006) 822–829.
[30] S. Altmeyer, V. Mathieu, S. Jullemier, P. Contal, N. Midoux, S. Rode, J.P. Leclerc, Comparison of different models of cyclone prediction performance for various operating conditions using a general software, Chem. Eng. Process. 43 (2004) 511–522.
[31] Fluent Incorporation, Fluent user's guide, second edition 4 (1997) 19–111.
[32] S.A. Morsi, A.J. Alexander, An investigation of particle trajectories in two-phase flow systems, J. Fluid Mech. 55 (1972) 193–208.